

Applying microscopy to the analysis of nuclear structure and function

Francisco Iborra,^a Peter R. Cook,^a and Dean A. Jackson^{b,*}

^a *Sir William Dunn School of Pathology, University of Oxford, South Parks Road, Oxford OX1 3RE, UK*

^b *Department of Biomolecular Sciences, UMIST, P.O. Box 88, Manchester M60 1QD, UK*

Accepted 15 October 2002

Abstract

One of the ultimate goals of biological research is to understand mechanisms of cell function within living organisms. With this in mind, many sophisticated technologies that allow us to inspect macromolecular structure in exquisite detail have been developed. Although knowledge of structure derived from techniques such as X-ray crystallography and nuclear magnetic resonance is of vital importance, these approaches cannot reveal the remarkable complexity of molecular interactions that exists *in vivo*. With this in mind, this review focuses on the use of microscopy techniques to analyze cell structure and function. We describe the different basic microscopic methodologies and how the routine techniques are best applied to particular biological problems. We also emphasize the specific capabilities and uses of light and electron microscopy and highlight their individual advantages and disadvantages. For completion, we also comment on the alternative possibilities provided by a variety of advanced imaging technologies. We hope that this brief analysis of the undoubted power of microscopy techniques will be enough to stimulate a wider participation in this rapidly developing area of biological discovery.

© 2003 Elsevier Science (USA). All rights reserved.

Keywords: Light microscopy; Electron microscopy; Live-cell imaging techniques; Advanced microscopy techniques

1. Introduction

If a picture really can replace 1000 words, recent innovations in microscopy have a bright future as it is now possible to explore how specific molecules function in living cells. This review provides a brief overview of how microscopy can be utilized as an approach to understanding cell function. We hope to guide the reader through this complex field while pointing out the advantages and limitations of particular techniques. To exemplify the demands of a particular technology the reader will be introduced to a limited range of basic experimental protocols. These, inevitably, cannot be treated exhaustively. Furthermore, as microscopy is used so widely it becomes impossible to provide a comprehensive appraisal of the various applications. Consequently, our discussion focuses on our own interests, structure–function relationships in mammalian

cell nuclei. For simplicity, we divide the techniques into two broad categories: light microscopy (LM) and electron microscopy (EM). LM is well suited to imaging living cells with low resolution, while EM provides high-resolution images of dead cells. Many routine techniques and applications will be familiar to readers, but beyond these lie specialized techniques that we will touch on to emphasize the range of alternatives available.

2. Methods

2.1. Light microscopy

Microscopes have been used to analyze tissues and cells since the early 17th century [1]. The fundamental basis of imaging in LM [2] is that light interacts with the sample and is magnified through a series of lenses prior to visualization. Visualization relies on contrast generated in the sample. For basic applications, white light can interact with a specimen that may or may not be

* Corresponding author. Fax: +44-161-236-0409.

E-mail address: dean.jackson@umist.ac.uk (D.A. Jackson).

stained, and different components of the light will be reflected, absorbed, or transmitted to generate an image. The interaction of light with the sample can be accentuated using techniques that depend on particular properties of the light such as its polarization, phase (e.g., in phase-contrast microscopy), or interference between phases (e.g., in differential interference contrast microscopy) and on particular properties of the sample (e.g., their fluorescence).

2.2. Immunofluorescence microscopy

Fluorescent molecules absorb light of a particular wavelength, become excited, and then lose the energy as light of longer wavelength (and lower energy). The difference between the peaks of excitation and the peaks of emission spectra is the Stokes shift (which is usually 10–20 nm). As the spectra of the excited and the emitted light differ, the two can be separated using appropriate filters. A specific advantage of this approach is that many colors can be imaged simultaneously.

Fluorescence technology can be applied to many aspects of cell biology, ranging from the analysis of cells and tissues to the behavior of single molecules [3]. For simplicity, attention here focuses on (i) the analysis of cellular distribution of specific molecules using indirect immunofluorescence and (ii) the use of fluorescent proteins to study distributions in living cells.

Indirect immunofluorescence is now used routinely to study cellular distributions. As examples, one might incorporate modified precursors (e.g., bromodeoxyuridine or bromouridine) into DNA or RNA and analyze the distribution of the resulting Br-DNA or Br-RNA and then compare it with the distribution of a protein participating in the synthesis of one or another nucleic acid. The basic steps include fixation to preserve the natural structure as far as possible (e.g., by incubation in 4–8%

paraformaldehyde for ~15 min). After removing the fixative, the distribution of the target molecule is revealed using antibodies tagged with fluorophores. Using transcription as an example, any Br-RNA might be visualized using a mouse anti-Br primary antibody followed by a fluorophore-conjugated secondary (i.e., an anti-mouse immunoglobulin). After washing to remove unbound antibodies and counterstaining the DNA (if desired), sites marked by the fluorescent secondary are imaged. The same principle can be applied to visualize the cellular distribution of any protein for which antibodies are available. Moreover, two or more target molecules can be immunolabeled within the same sample if appropriate antibodies—developed in different species—are available (Fig. 1). Examples of typical approaches are described by Iborra et al. [4] and Pombo et al. [5].

Images such as those shown in Fig. 1 are usually prepared on cells grown or fixed on to a suitable surface, commonly glass. Because of this the images are usually derived from whole-cell mounts or tissue slices. It is worth noting that for certain applications image quality is improved if samples are prepared as cryosections [5]. Here, cells might be fixed as a pellet, washed, and equilibrated with 2.1 M sucrose. The pellet is transferred on to a copper block, shaped into a cone with forceps, and frozen by immersion in liquid nitrogen. Now the pellet is hard enough to be cut on a cryomicrotome to give sections of 100–500 nm that can be transferred to slides for immunostaining and imaging (Fig. 2). This has significant advantages. For LM, reducing the thickness of the specimen can eliminate extraneous signal that in whole mounts might originate outside the focal plane. More helpfully, the same blocks can be used to generate samples that can be processed for both LM and EM (see below) techniques [5].

The major limitation of LM in cell biology is the resolution (R), which is defined by Eq. (1)

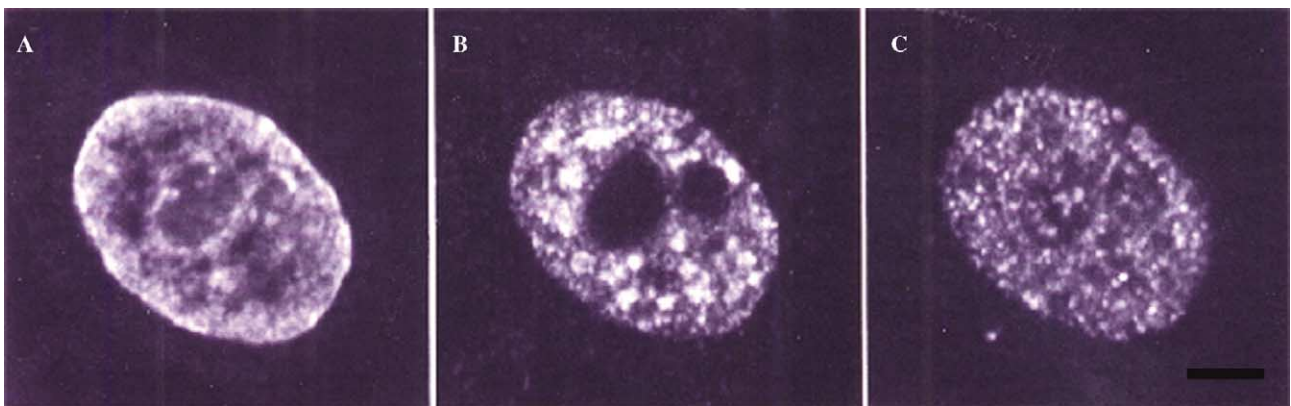


Fig. 1. Nuclear compartments by confocal microscopy. HeLa cells growing on glass were permeabilized in an isotonic buffer and transcription was performed for 15 min in the presence of BrUTP. Samples were fixed and immunolabeled from Br-RNA-containing sites (C) and sites containing the autoimmune antigen Sm (B). DNA was counterstained with TOTO3 (A). (A)–(C) show the three labels revealed in a single confocal section of 700 nm. Note the distribution of condensed and open chromatin (A), the classical “speckled” distribution of the Sm protein (B), and the complexity of the transcription sites (C). Nucleus has a diameter of 10 μ m. See [53] for details. With permission of Academic Press.

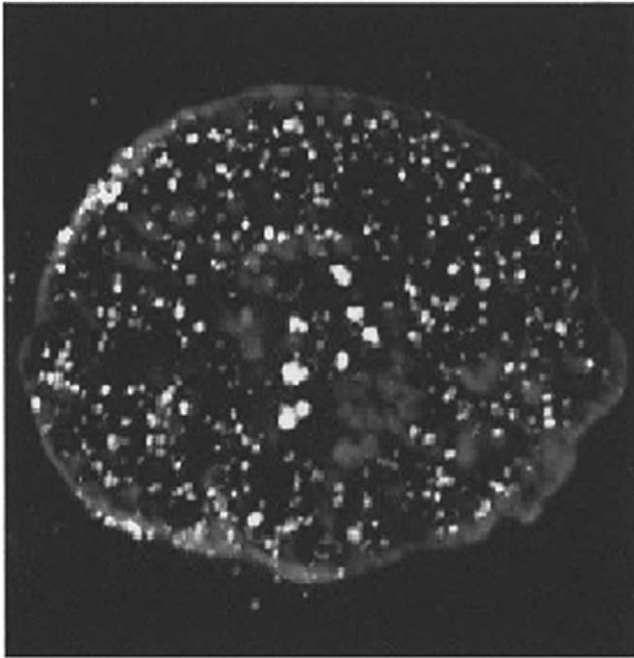


Fig. 2. Distribution of transcription sites using cryosections for LM. HeLa cells were permeabilized, nascent transcripts were extended in BrUTP, and cryosections (~ 90 nm) were prepared. Br-RNA was indirectly immunolabeled with Cy3 and nucleic acids were counterstained with TOTO-3. Red and far-red images were collected using a “confocal” microscope and images prepared without background subtraction (thresholding). Note the distribution of very bright nucleolar foci in the center and many small foci throughout the nucleoplasm. TOTO-stained heterochromatin is also clearly visible around the nucleolus and along the nuclear periphery. Reproduced from [5] with permission of Oxford University Press.

$$R = \frac{0.61\lambda}{\text{NA}}, \quad (1)$$

where λ is the wavelength of light, and NA is the numerical aperture of the objective. For most applications, a lens with a NA of ~ 1.3 is used, so resolution approximates to $\lambda/2$, which is typically 250–300 nm for visible light. Many subcellular structures are smaller than this and so cannot be resolved one from another. However, it is important to distinguish resolution from spatial precision as modern instruments allow definition of the position of a signal to within a few nanometers. Hence, in a dynamic experiment a fluorescence particle or gold bead might be tracked by fluorescence or video enhanced microscopy to within ~ 10 nm, while in a static experiment a labeled structure might be localized relative to another to within ~ 20 nm by simple confocal microscopy [6] and ~ 2 nm by 4Pi-confocal microscopy [7].

In routine LM, image quality can be degraded by four independent phenomena: noise, scatter, glare, and blur [8]. We are all familiar with the noise in our (broadcast) analog TV images during bad reception. Noise is quasirandom because its statistical distribution

can be predicted if the mechanics of its source is known. In digital microscopy, the source is the signal itself (the photon shot noise) or the imaging system. Signal-dependent noise has a Poisson distribution, while imaging-system noise usually has a Gaussian distribution, so both can be removed using the appropriate filters. Scatter gives a random distortion, and results from the disturbance of light as it passes through regions of the specimen with different refractive indices; the thicker and more heterogeneous the specimen, the more scatter there is. Unfortunately, no completely satisfactory method exists that enables us to predict how a particular sample scatters. Glare is also random, but occurs in the lenses and filters of the imaging system rather than in the specimen; it is minimized using antireflective coatings. Blur results from the nonrandom diffraction of light as it passes through the system; much of it comes from out-of-focus light emanating from above and below the focal plane. It limits resolution—an image whose resolution is limited only by blur is known as “diffraction limited.” As we have sophisticated explanations of blur, and as it is characteristic of the microscope system (mainly the objective lens) and not the sample, it can be modeled easily. Various deconvolution algorithms are now available; they use a model of the imaging process to either subtract or reassign out-of-focus blur and so improve the contrast and resolution of digital images. Deconvolution is sometimes described as an alternative to confocal microscopy (see below), but this is not strictly true, as confocal images can also be deconvolved. However, most users apply deconvolution to a stack of images collected on a wide-field microscope to generate images with resolution comparable to those obtained with the confocal microscope. Wallace et al. [8] have written an excellent guide to deconvolution and its pitfalls.

Laser scanning confocal microscopy provides a different way of removing out-of-focus blur; only emitted light that passes through a pinhole aperture that is confocal with the focal plane in the specimen is collected, while out-of-focus blur is discarded [9,10]. The introduction of a pinhole also improves lateral resolution, as the aperture can be reduced so that the photomultiplier operates as a coherent point detector. Under ideal circumstances this delivers a superresolution that is ~ 1.4 -fold better than that obtainable by conventional optical microscopy. In confocal microscopy the sample is also illuminated with a scanning laser beam of specific wavelength and not with filtered light from the broad spectrum source (e.g., a mercury or xenon lamp) used in conventional microscopes. Despite the expense of the lasers and confocal scan head, confocal microscopy has been in wide use for ~ 20 years.

Recently, spectral analyzers have been added to commercially available confocal microscopes. The Leica TCS SP2 system applies a filter-free spectrophotometer

to each detector channel, which allows customization of emission parameters to maximize sensitivity and minimize cross talk. More recently, Zeiss introduced the META spectrophotometer for their LSM510 confocal microscope. After the emitted light has passed through the confocal aperture, the META attachment separates it into its spectral components and so into an array of 32 photomultipliers (each covering 11 nm). The spectral information obtained can then be compared with the spectral signature of any fluorophores in the specimen to allow pure images to be resolved. This powerful technology allows fluorophores with peak emissions that differ by ~ 10 nm to be distinguished (e.g., fluorescein isothiocyanate and green fluorescent protein (GFP)).

Many confocal beams are combined together in the UltraView system (Perkin–Elmer) which uses an array of sources in a Nipkow disk rather than a single scanning beam; this permits rapid image acquisition (i.e., over tens of milliseconds) of weakly fluorescent objects, which can be needed when analyzing small molecule signaling [11,12]. Modifications of the multifocal principle—such as aperture correlation, time-multiplexed microscopy, and multifocal multiphoton microscopy—can also deliver superior axial resolution [13].

2.3. Live-cell imaging

The recent development of techniques to image molecules in living cells represents a revolution in cell biology [14]. The traditional approach was to introduce (e.g., by microinjection or transfection) fluorescently tagged molecules into cells, make a movie of the cell, and analyze the dynamics of the fluorescent structures in successive frames [15]. However, the most significant single development has been the introduction of small autofluorescent proteins (e.g., the GFP from the jellyfish *Aequorea victoria*) that can be coupled to a protein of interest to generate a fluorescent hybrid protein. The composite can then be expressed and studied in living cells, where information about its spatial distribution can provide compelling insights into cellular function. In many cases, such hybrid proteins function normally and can replace their natural counterparts so that their distributions can be followed as cells grow and divide. As with all fluorochromes, the main practical problem in imaging GFP in living cells is the phototoxicity of the illuminating light; thus, experiments are usually a compromise between using enough light to obtain a suitable image, but not too much to compromise the cell [14]. Finally, video microscopy adds many complexities (for a review, see [15]).

2.4. FRAP, FLIP, and FRET

Protein dynamics in living cells can be monitored using fluorescence reactivation after photobleaching and

fluorescence loss in photobleaching. In FRAP, a region of the cell containing the fluorescent protein (or other fluorescent molecule) is irradiated to bleach the fluorochrome. The fluorescence intensity in the bleached area is then monitored to establish how quickly still-fluorescent molecules in unirradiated areas equilibrate with their now nonfluorescent counterparts in the bleached zone. Small proteins that diffuse rapidly will equilibrate within seconds, larger proteins equilibrate more slowly, and any protein stably bound to other structures (e.g., the histones) can take many hours before equilibrating completely. This approach measures dynamics locally. FLIP is a complementary approach. A selected region of a cell is irradiated repeatedly, while fluorescence in a neighboring unbleached region is monitored; the intensity in the unbleached region falls progressively as fluorescent molecules diffuse away into the bleaching zone. RNA binding proteins tagged with GFP have been examined using these techniques [16].

Fluorescent resonance energy transfer allows the spatial arrangement of fluorochromes to be assessed in living cells. FRET is an interaction between excited states of two fluorochromes lying ~ 5 nm apart in the appropriate orientation so that energy is transferred from one to the other without emission of a photon. The efficiency of energy (E) transfer during FRET is given by

$$E = 1/1 + (R/R_0)^6, \quad (2)$$

where R is the distance between the donor and the acceptor and R_0 is the distance when 50% of the energy is transferred. The relative orientation of the two fluorochromes also influences R_0 . As FRET efficiency falls off with the sixth power of the distance between the two fluorochromes, energy transfer is ideally suited to measure molecular interactions in the range 1–10 nm. As a result, the molecular “touching” of two fluorescent probes can be detected, even though the distances involved are well below the resolution of LM. Consider two fluorescent variants of the green fluorescent protein—the cyan and yellow variants. Only the cyan variant is excited by light of 433 nm to fluoresce at 476 nm. If the yellow variant lies very near by, some energy is transferred to it, and less energy is emitted at 476 nm. However, the transferred energy is emitted at a longer wavelength (i.e., 527 nm) characteristic of the yellow “acceptor.” For some applications in cell biology, it is impractical to measure FRET directly as the FRET signal may be too low compared to the normal fluorescence emission from the donor fluorophore, and it is often difficult to eliminate completely the excitation of the acceptor molecule. These problems are circumvented by employing the techniques of acceptor or donor photobleaching [17], as in a study of the interactions of p53 with the nuclear matrix [18]. Confocal images are first acquired using donor and acceptor fluorescence; then, the acceptor in one area of the cell is bleached with

a laser, and a second donor fluorescence image is captured. Destroying the acceptor enhances the donor signal (as energy can no longer be lost by FRET to the acceptor) so the intensity of FRET can be calculated pixel by pixel.

2.5. *Fluorescent speckle microscopy (FSM)*

Cell biologists usually try to increase the number of fluorescent molecules in the cell to increase the signal. However, this is often not the best strategy as many fluorochromes may not be incorporated into the structure of interest and so give a high background; they also contribute to the out-of-focus blur. FSM uses the strategy of reducing the number of fluorescent molecules, so that only a few are assembled with endogenous unlabeled subunits into the structure [19,20]. With this in mind, it is important to remember that modern, light-efficient microscopy equipment can detect single fluorophores under ideal conditions *in vitro* and 5–10 fluorophores within a diffraction-limited region of a specific cell structure *in vivo*.

FSM is perfectly suited to the analysis of molecular dynamics in living cells. An excellent example of the power of this approach [19] is in the study of microtubule flux in mitotic spindles—in mammalian cells it is extremely difficult to resolve individual microtubules by fluorescence microscopy. In one frame of a time-lapse movie, the structure containing enough molecules to be seen appears as a speckle, and the appearance, disappearance, and movement of the speckles in subsequent frames yields dynamic information. FSM images are usually captured using a conventional wide-field microscope; they have low backgrounds and little out-of-focus blur, and they can be collected in thick regions of living cells. Another significant advantage is that the low level of fluorescent protein is less likely to perturb protein balances in the cell.

2.6. *Fluorescence correlation spectroscopy (FCS)*

FCS is a technique for monitoring the random motion of fluorescently labeled molecules in a defined volume irradiated by a focused laser beam [21]. The fluctuations in position provide information on the rate of diffusion and so mass. Because the underlying principle is so simple, FCS is ideally suited to studying molecular interactions in cells and has provided, for example, compelling insights into the dynamics of mRNA movement in the nuclei of mammalian cells [22]. This technology requires low concentrations of fluorochromes.

2.7. *Multiphoton microscopy*

A fluorophore can be excited by absorption of a single photon of light at a specific wavelength, and then

subsequent decay produces the fluorescence. Unfortunately, fluorochromes can also be bleached during the exposure, and some of the products produced by the bleaching are toxic. With both conventional and confocal microscopy, photobleaching occurs throughout the depth of the sample and the loss of fluorescence by the probe and the toxicity both limit the number of recordings that can be made.

Multiphoton microscopy provides an alternative that reduces these problems [23]. In the simplest case, two-photon microscopy, the dye molecule is excited by the simultaneous absorption of two photons each with about one half the energy normally used for excitation. The efficiency of two-photon adsorption is proportional to the square of the illumination intensity, which means that the intensity of illumination can be made sufficiently high to excite two-photon fluorescence only in the focal plane (Fig. 3). This gives an essentially confocal output without the use of a confocal aperture. Additionally, as two-photon excitation occurs only at

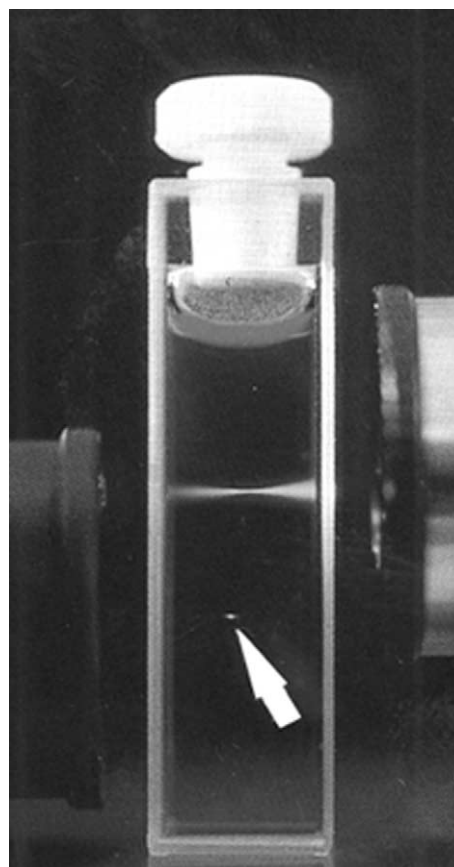


Fig. 3. Principle of multiphoton microscopy. This image demonstrates how light irradiates throughout the depth of a sample under LM epifluorescence but activates fluorescence only at the focal point of the laser (arrow) under two-photon absorption. The cuvette filled with a safranin solution is illuminated with green light (532 nm) through a low NA lens, top and right, and infrared light (1047 nm, from a mode-locked neodymium–yttrium lanthanum fluoride laser), bottom and left. Photograph courtesy of Brad Amos, MRC Cambridge.

the focus, other parts of the sample are bleached less, and phototoxicity is reduced accordingly. Another advantage is that the near-infrared light used for two-photon illumination is able to travel deeper into a sample, so allowing images to be generated from samples many cells deep. A potential disadvantage is the damaging effects of heat generated by the high-powered laser light at the focal point. Such heating is lessened by using pulsed lasers where the pulses are separated by roughly the fluorescence lifetime of the fluorochrome (i.e., a few nanoseconds).

2.8. Fluorescence lifetime imaging (FLIM)

A common goal in cell biology is to study interactions between molecules in the living state. We saw above how FRET can be used to address this. A related analysis involves measurement of the fluorescence lifetime of the donor fluorophore. As the kinetics of decay of the activated state depends on whether or not a FRET donor is engaged in productive interactions, FLIM data can be used to calculate true FRET efficiencies and confirm the existence of molecular interactions in living cells [17].

2.9. Improving LM resolution

The point spread function (PSF) of the light emanating from any fluorophore in the light path of a microscope is a product of the lenses that contribute to image formation. With both epifluorescence and confocal microscopy, resolution is anisotropic, and about threefold lower along the optical (z) axis (i.e., ~ 700 nm). Quite clearly, diffraction-limited resolution significantly restricts the use of LM for certain biological applications, where structures much smaller than the theoretical resolution capabilities are often studied. In the z axis, this resolution problem presents an even greater handicap which can severely limit 3D data analysis. Axial tomography improves this resolution; a 3D image is reconstructed from a series of data sets in which the sample has been rotated under the microscope to obtain a series of views in which the axis of reduced resolution is varied. This technique can be applied to wide-field and confocal microscopy, when samples can be prepared in such a way that a series of data sets can be obtained. The usual way of achieving this is to mount the sample in or on the surface of a glass capillary which can then be rotated as the data are acquired (this is equivalent to stereo techniques used in EM). Using only three data sets generated in this way clearly improved the resulting image [24].

Various other systems that provide significant improvements in resolution have been devised. Techniques such as these are ideally suited to the analysis of sub-nuclear compartments, such as chromosome territories.

Although these instruments are very specialized and not commercially available we feel that it is important for the reader to be aware of the available options.

4Pi. The poor z resolution stems from anisotropy of the emitted light, which can be reduced by increasing the illuminating aperture so that the sample is bathed within a complete converging sphere of light. Although this is not possible in practice, 4Pi microscopy uses two aligned and opposed objectives to increase angular coverage and so the axial resolution [7,25].

Theta. Another solution to the anisotropy problem is to use two objectives such that the axes of the collection optics are offset relative to the illumination path by an angle (θ) which is generally $\sim 90^\circ$; this improves axial resolution because the PSFs of the illumination and detection optics differ [26].

I⁵M. A sevenfold improvement in axial resolution has been achieved in 3D wide-field fluorescence microscopy by illuminating and/or observing from both sides simultaneously; interference effects in the excited and the emitted light provide higher-resolution axial information [27].

Spatially modulated microscopy. A far-field laser fluorescence microscope uses two objectives to generate interference patterns that yield a ~ 10 -fold increase in spatial resolution. Though sophisticated, it is clear that this approach has the capability to generate topological measurements that would be classically regarded as beyond the capabilities of light microscopy [28].

2.10. Advanced LM imaging systems

To complete our analysis of the use of fluorescence in light microscopy we would like to note the specialized application of the following advanced imaging techniques.

2.10.1. Total internal reflection fluorescence microscopy

Total internal reflection occurs when light propagating in a dense medium (such as glass) meets an interface with a less dense medium (such as water). If the light meets the interface at a small angle, some of the light passes through the interface and some is reflected. At the critical angle—which depends on the refractive indices of the media—all light is reflected. However, some energy beams propagate a few hundred nanometers into the aqueous sample, generating an evanescent wave that is capable of exciting local fluorophores. This technique generates fluorescence with an extremely low background of excitation light and so is amenable to single molecule analyses where sensitivity and a high signal:noise ratio are required [29,30].

2.10.2. Near-field optical microscopy

This technique employs a sharp optical probe (laser light ~ 10 nm wide) which is scanned over the object.

Resolution is determined by the size of the probe and the probe–sample distance. In idealized circumstances this approach is capable of delivering resolution below 10 nm. However, near-field techniques are specialized, and technically demanding, and of limited scope for the analysis of biological preparations.

2.10.3. Scanning near-field optical microscopy

This modification has certain advantages. A point light source close to the sample is used for scanning, and the scattered or transmitted light is recorded point by point across the sample; then, optical images can be generated with a resolution that is not limited by diffraction. This technique has been applied to routine high-resolution fluorescence imaging [31].

2.10.4. Optical far-field microscopy

As noted above, resolution is determined by the diffraction properties of the light used. However, a substantial improvement in optical resolution is possible if specific features or distinct volumes of the sample differ in optical properties such as the emission or absorption spectrum or the lifetime of the excited state. With this technology, spectrally selective imaging of single molecules at cryogenic temperatures (generated using liquid helium) provides a lateral resolution that is at least an order of magnitude beyond the diffraction limit of light in all three spatial dimensions. In the best-case scenario an unprecedented single-molecule lateral resolution of 3.4 nm has been described [32]. However, we are still a long way from achieving this kind of resolution in living cells.

3. Electron microscopy

As we have seen, the operational resolution of LM is usually ~ 250 nm. If higher resolution is demanded, EM is capable of delivering a resolution of ~ 0.2 nm. However, as the sample is imaged in a vacuum, it must be well fixed, usually using chemicals such as formaldehyde and glutaraldehyde that react with primary amine groups on neighboring molecules to cross-link them into a gel [33]. A typical procedure involves successive light (4% formaldehyde for 10 min on ice), which stops all enzymatic activities, and harsh fixation (8% formaldehyde for 50 min). The fixed cells are then embedded in a medium (resin) that is hard enough to be cut into ultrathin sections (30–120 nm thick). The resin used for routine EM is determined by the specific demands of individual experiments; epoxy resins can be processed and stained to give outstanding morphology but poor immunolabeling, while nonepoxy resins (e.g., LR white) give poorer morphology but better immunolabeling (below). Cryosectioning provides an alternative approach [5] (see above).

3.1. Immunolabeling

Immunolabeling techniques fall into two broad categories: (1) postembedding immunolabeling on sections and (2) preembedding immunolabeling on cells prior to embedment in the resin. In both cases, samples may be “blocked” to prevent nonspecific binding and incubated first with a primary antibody to the molecule of interest and second with a secondary antibody that specifically interacts with the primary antibody. The secondary is conjugated with gold particles of 1–20 nm diameter, and the use of secondaries with differently sized particles allows the distribution of two targets in one sample to be compared (Fig. 4). (For further details, see [4,5,34].) Unfortunately, antibodies added after embedding have limited access to the interior of the section and so bind mainly to antigens exposed on the surface; this inevitably reduces labeling intensity. In addition, the process of embedding in Epon—particularly during dehydration and polymerization—can extract and/or destroy antigens [33]. In contrast, preembedding labeling can provide improved antibody binding, but poorer morphological clarification. Therefore, different techniques are used for different purposes. For example, antigens such as bromine (in Br-RNA) or biotin that survive the rigors of

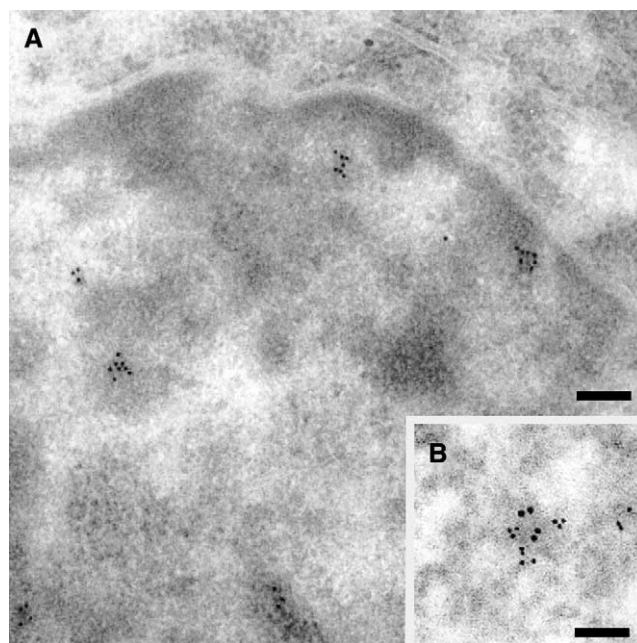


Fig. 4. Preserving morphology in immuno-EM. Under some circumstances it is possible to perform efficient immunolabeling while preserving morphology. BrUMP incorporated into RNA provides an excellent example, as the Br-RNA target epitope is resistant to fixation and very abundant. This means that samples can be labeled on the surface of Epon sections to give adequate labeling and good morphology. (A) Distribution of Br-RNA-containing sites in a section generated from a Br-labeled HeLa cell nucleus; (B) a double-labeled transcription factory immunostained for RNA polymerase II (large gold) and Br-RNA (small gold). Bar 50 nm (B).

Epon embedding can be detected efficiently by postembedding immunolabeling (Fig. 5) [4], while others (e.g., protein antigens) cannot. Then, resins (e.g., LR White, Lowicryl K4M) permitting better postembedding immunolabeling can be used, but with a concurrent degradation of morphology. Cryosections have some advantages; antibodies can penetrate more easily into the center, and antigenicity may be preserved better because samples are not dehydrated with alcohols [5]; however, the technique demands some technical expertise to preserve perfect morphology and so it is not widely used [33].

Various problems are associated with interpreting images of immunolabeled structures, especially when those structures are small. First, the relationship between signal intensity (i.e., the density of gold particles) and target concentration is often not linear as the target epitopes can soon become saturated with antibodies [33]. Second, gold particles can often lie tens of nanometers away from the target epitopes that they mark; for example, a common procedure uses 10-nm particles connected through primary and secondary immunoglobulin type G molecules with lengths of ~ 9 nm [35]. Third, in double immunolabeling, one antibody can block access of another to its target [5]. Fourth, numerical analysis relies heavily on stereology, which deals with quantitative aspects of shape, size, number, and

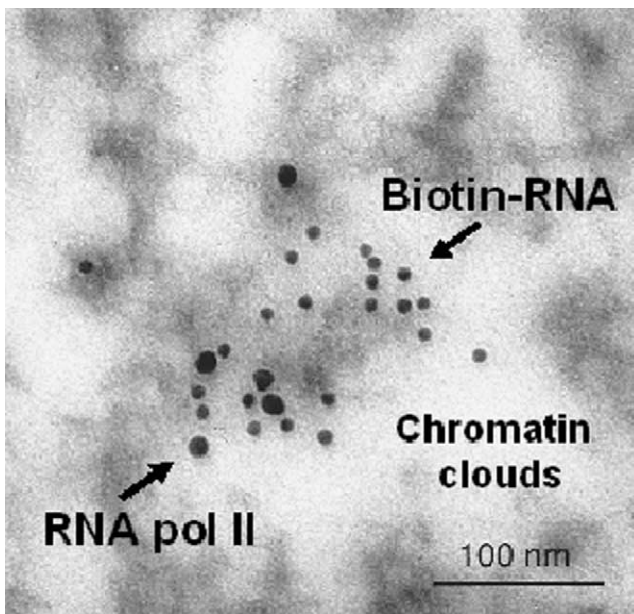


Fig. 5. High-efficiency immuno-EM. EM immunolabeling is a routine approach to analyze protein distributions at high resolution. This example shows a section prepared in LR-white that has been treated using the EDTA regressive staining technique and immunolabeled using antibodies to the active form of RNA polymerase II and biotin-RNA (labeled in vitro using biotin-CTP). Note the relative distributions of RNA polymerase II (large, 10 nm, gold particles), biotin-RNA (small, 5 nm, gold particles), chromatin clouds (pale areas), and RNA-rich interchromatin channels (gray areas). Note that with this technique immunolabeling is good but morphology is compromised.

orientation in space [36], and many biologists find this kind of analysis difficult. The analysis of transcription centers in mammalian cells provides a good example of the value of stereological techniques [34,37].

3.2. Specific cytochemical methods

Over the years, a range of cytochemical techniques for staining specific cytochemical targets have been developed. As an example, we focus on methods relating to nucleic acids; details of other procedures are described by Lewis and Knight [38].

The methylation-acetylation procedure for staining nucleic acids is compatible with immunolabeling and in situ hybridization. A mixture of methanol and acetic anhydride is used to methylate the carboxyl groups in proteins and amino acids; this reaction efficiently blocks protein staining and enhances the contrast of nucleic acids stained with uranyl acetate [39]. DNA-containing structures can also be revealed using osmium amine B; DNA is hydrolyzed to give aldehyde groups that can bind the osmium [40]. Furthermore, RNA can be detected using EDTA regressive staining [38] or terbium [41].

3.3. Alternative approaches

The techniques described above are generally applied to whole cells or tissue samples, but a wide range of alternatives is available. For example, where 3D information is required, cells may be grown directly on coated grids and treated on the grids as whole mounts [42]. Alternatively, cells can be extracted, embedded in a removable wax, cut into thick sections (100–500 nm), and imaged after removing the wax [43]. The combination of resinless EM technology with chromatin extraction techniques, using cells encapsulated in agarose microbeads, provides an excellent opportunity to reveal dispersed cellular structures such as those of the nucleoskeleton [43]. In other cases, cells are disrupted and placed directly onto grids for imaging, as in “Miller spreads,” which allow visualization of genes in action [44]. Fig. 6 illustrates a variant of this approach. Purified proteins and large protein complexes such as large heterogeneous nuclear RNA particles [45] and nuclear pores [46] can also be analyzed using sophisticated EM-based tomography techniques.

3.4. Instrumentation

As with LM, many commercial machines are available. These are commonly classified into scanning or transmission machines, and for most purposes the latter provide the most valuable information. However, high-power scanning machines, such as the field emission in lens scanning electron microscope (FEISEM), can pro-

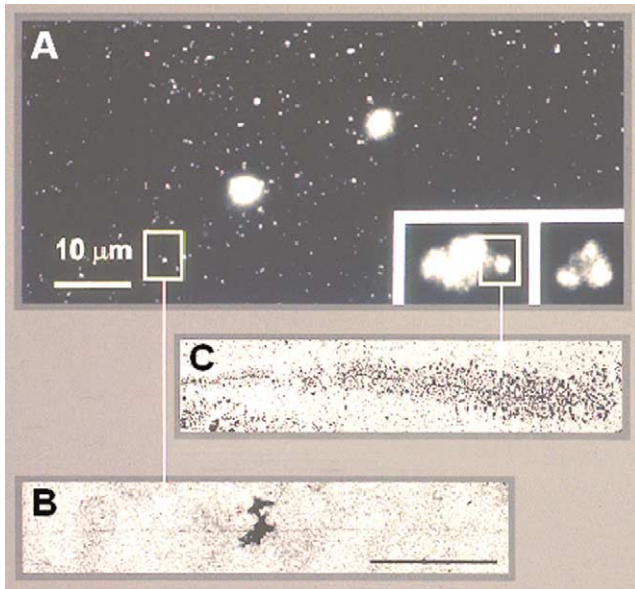


Fig. 6. EM spreading techniques. HeLa cells labeled with BrUTP were extracted with sarkosyl and spread over a glass slide, and some of the spread was deposited onto “sticky” nickel grids (coated with Formvar and carbon and then with 30 mg/ml ethidium bromide [54]). After drying, samples on either the slide or the grid were fixed and immunostained. LM (A) reveals two populations of Br-RNA-containing foci [37], shown by drug inhibition to be derived from RNA polymerase II activity (numerous small foci) or RNA polymerase I activity fewer very bright foci; see inset in (A). Transcript density shown by EM (B, C) shows that the nucleolar genes (C) have typically about 100 engaged transcripts [44], whereas the protein-coding genes (B) generally have 1–3 [37]. Reproduced with permission from the American Society for Cell Biology and Scandinavian University Press.

vide high-quality images at high magnification [47] (Fig. 7). Electron spectroscopy imaging (ESI) utilizes energy-filtered, inelastically scattered electrons to generate images that contain both mass density and ana-

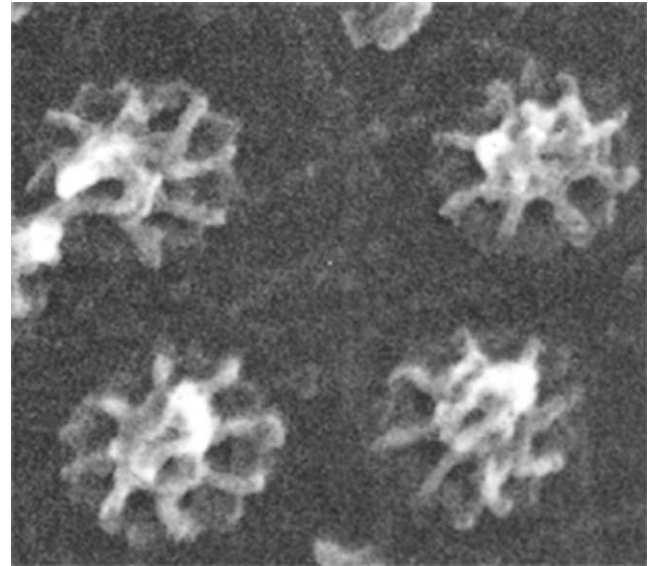


Fig. 7. Nuclear pore structure by FEISEM. FEISEM provides a very powerful technique to study the organization of complex structures such as the nuclear pore. This example shows the view of pores from the nucleoplasmic face of a nuclear membrane isolated from a *Xenopus laevis* oocyte. Note, however, that this cell is especially amenable to the isolation of nuclear membranes and that it is not usually possible to generate such clear images from nuclear membranes of somatic mammalian cells. Reproduced from [55] with permission of Rockefeller University Press.

lytical information [48]. It provides an elemental analysis technology and allows molecules that are rich in particular elements to be identified. For example, the spatial distribution of nucleic acids can be mapped by their phosphorus content, which is much higher than that of any surrounding proteins [49] (Fig. 8). Unfortunately, ESI requires a specially adapted electron microscope that is not widely available.

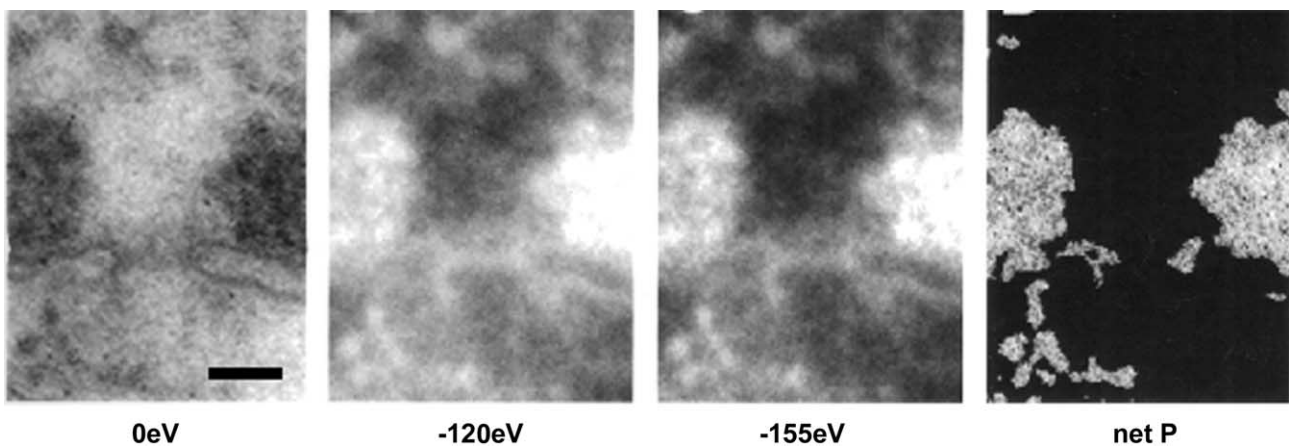


Fig. 8. ESI to investigate nuclear export. ESI of HeLa nuclei can be used to map the location of RNP particles passing through nuclear pores. Using the Zeiss 912 microscope, images are captured using filtered electron beams of appropriate energies, here 0, –120, and –155 eV, and intensity profiles are processed to calculate the intensity due only to phosphorus atoms, net P. The image shows a single nuclear pore with two associated RNP complexes. Note the position of heterochromatin lying against the nuclear lamina, but not covering the pore. Ribosomes associated with endoplasmic reticulum are clearly visible in the cytoplasm. Bar, 100 nm. Reproduced from [49] with permission of The Company of Biologists Ltd.

4. Alternative imaging techniques

We have seen that LM is ideally suited to the study of living cells and tissues, whereas EM demands that the tissue is fixed and, for most applications, dehydrated and stained. A less destructive alternative to EM is provided by soft X-ray microscopy. Here, photons of ~ 520 eV (corresponding to a wavelength of 2.4 nm) can yield high-contrast images of thick (up to ~ 10 μm) hydrated samples at better than 50-nm resolution [50]. Coupled with immunolabeling, this technology provides 3D information about the distribution of proteins in whole, hydrated cells with resolution that is greater than fivefold better than that routinely attainable using LM.

The scanning probe principle described above is also used in scanning force microscopy (SFM). Here, a sharp tip mounted at the end of a flexible cantilever is used to scan the topography of a sample deposited on a flat surface such as a glass slide. The tip is moved laterally across the sample and the displacement as it moves across the sample interpreted to generate an impression of the surface structure. In an alternative to this scanning mode, called tapping mode, the cantilever is oscillated near its resonance frequency during lateral scanning of the sample. As the probe passes over the sample, changes in the amplitude of oscillation are induced. This signal is then used in feedback to keep the amplitude constant throughout the scan. SFM provides surface detail with a level of resolution in the nanometer range; hence this technology is amenable to the analysis of structures such as a chromatin fiber. This delivers a resolution approaching that of classical EM techniques but with the significant advantage that imaging can be performed in air at room temperature and humidity, so that the sample preserves a layer of liquid and is not extensively damaged by drying [51,52].

5. Concluding remarks

One of the ultimate goals of biological research is to understand the mechanisms that drive cell function within the living organism. With this goal in mind, a wide range of sophisticated technologies that allow us to inspect macromolecular structure in exquisite detail has been developed. But while knowledge of structure derived from techniques such as X-ray crystallography and NMR is of vital importance they are unable to provide information about molecular function as it pertains to the living cell. Where living cells are concerned, microscopy techniques remain the analytical tool of choice. This review attempts to provide an overview of the wide variety of microscopy techniques that can be applied to the analysis of cell structure and function. In doing this, we have attempted to provide enough detail to allow the reader to recognize the enormous potential of this

technology without confounding her/him with technical detail. We hope that this taste of the capabilities of microscopy techniques will be enough to stimulate a wider participation in this rapidly developing sphere of biological investigation.

References

- [1] H. Harris, *The Birth of The Cell*, Yale University Press, New Haven, CT, 1999.
- [2] A.J. Lacey (Ed.), *Light Microscopy in Biology: A Practical Approach*, IRL Press, 1989.
- [3] T. Ha, *Methods* 25 (2001) 78–86.
- [4] F.J. Iborra, D.A. Jackson, P.R. Cook, *Science* 293 (2001) 1139–1142.
- [5] A. Pombo, D.A. Jackson, M. Hollinshead, Z. Wang, R.G. Roeder, P.R. Cook, *EMBO J.* 18 (1999) 2241–2253.
- [6] E.M.M. Manders, J. Microsc. 185 (1996) 321–328.
- [7] M. Schmidt, M. Nagorni, S.W. Hell, *Rev. Sci. Instrum.* 71 (2000) 2742–2745.
- [8] W. Wallace, L.H. Schaefer, J.R. Swedlow, *BioTechniques* 31 (2001) 1076–1097.
- [9] C.J.R. Sheppard, D.M. Shotton, *Confocal Laser Scanning Microscopy*, Bios Scientific Publishers, 1997.
- [10] S.W. Paddock, *Confocal Microscopy: Methods and Protocols*, Humana Press, Clifton, UK, 1999.
- [11] A. Toker, L.C. Cantley, *Nature* 387 (1997) 673–676.
- [12] S.J. Isakoff, T. Cardozo, J. Andreev, Z. Li, K.M. Ferguson, R. Abagyan, M.A. Lemmon, A. Aronheim, E.Y. Skolnik, *EMBO J.* 7 (1998) 5374–5387.
- [13] A. Enger, V. Andresen, S.W. Hell, *J. Microsc.* 206 (2001) 24–32.
- [14] M. Chalfie, S. Kain (Eds.), *Green Fluorescent Protein, Properties, Applications and Protocols*, Wiley-Liss Publications, New York, 1998.
- [15] S. Inoué, K.R. Spring, *Video Microscopy*, second ed., Plenum Press, New York, 1997.
- [16] T. Misteli, *Science* 291 (2001) 843–847.
- [17] F.S. Wouters, P.J. Verveer, P.I.H. Bastiaens, *Trends Cell Biol.* 11 (2001) 203–211.
- [18] A.L. Okorokov, C.P. Rubbi, S. Metcalfe, J. Milner, *Oncogene* 21 (2002) 356–367.
- [19] C.M. Waterman-Storer, E.D. Salmon, *FASEB J. (Suppl. 2)* (1999) S225–S230.
- [20] T.J. Keating, G.G. Borisy, *Curr. Biol.* 10 (2000) R22–R24.
- [21] P. Schwille, *Cell. Biochem. Biophys.* 34 (2001) 383–408.
- [22] J.C. Politz, E.S. Browne, D.E. Wolf, T. Pederson, *Proc. Natl. Acad. Sci. USA* 95 (1998) 6043–6048.
- [23] K. Konig, *J. Microsc.* 200 (2000) 83–104.
- [24] R. Heintzmann, C. Cremer, *J. Microsc.* 206 (2001) 7–23.
- [25] S.W. Hell, M. Schrader, H.T.M. van der Voort, *J. Microsc.* 87 (1997) 1–7.
- [26] S. Lindek, C. Cremer, E.H.K. Stelzer, *Appl. Opt.* 35 (1996) 126–130.
- [27] M.G.L. Gustafsson, D.A. Agard, J.W. Sedat, *J. Microsc.* 195 (1999) 10–16.
- [28] B. Albrecht, A.V. Failla, A. Schweitzer, C. Cremer, *Appl. Opt.* 41 (2002) 80–87.
- [29] D. Axelrod, *Traffic* 2 (2001) 764–774.
- [30] D. Toomre, D.J. Manstein, *Trends Cell Biol.* 11 (2001) 298–303.
- [31] A.J. Meixner, H. Kneppel, *Cell Mol. Biol.* 44 (1998) 673–688.
- [32] A. Bloeb, Y. Durand, M. Matsushita, H. van Dermeer, G.J. Brakenhoff, J. Schmidt, *J. Microsc.* 205 (2002) 76–85.
- [33] G. Griffiths, *Fine Structure Immuno-Cytochemistry*, Springer, Berlin, 1993.

- [34] F.J. Iborra, D.A. Jackson, P.R. Cook, *J. Cell Sci.* 109 (1996) 1427–1436.
- [35] F.J. Iborra, P.R. Cook, *J. Histochem. Cytochem.* 46 (1998) 985–992.
- [36] E.R. Weibel, *Stereological Methods, Volume 2 “Theoretical Foundations”*, Academic Press, New York, 1980.
- [37] D.A. Jackson, F.J. Iborra, E.M. Manders, P.R. Cook, *Mol. Biol. Cell* 9 (1998) 1523–1536.
- [38] P.R. Lewis, D.P. Knight, Staining methods for sectioned material, in: A.M. Glauert (Ed.), *Practical Methods in Electron Microscopy*, North-Holland, Amsterdam, 1977.
- [39] P.S. Testillano, P. Gonzalez-Melendi, P. Ahmadian, M.C. Risueno, *J. Struct. Biol.* 114 (1995) 123–139.
- [40] M. Biggiogera, J.L. Courtens, M. Derenzini, S. Fakan, D. Hernandez-Verdun, M.C. Risueno, M.O. Soyer-Gobillard, *Biol. Cell* 87 (1996) 121–132.
- [41] M. Biggiogera, S. Fakan, *J. Histochem. Cytochem.* 46 (1998) 389–395.
- [42] J.A. Nickerson, *J. Cell Sci.* 114 (2001) 463–474.
- [43] P. Hozak, A.B. Hassan, D.A. Jackson, P.R. Cook, *Cell* 73 (1993) 361–373.
- [44] Y.N. Osheim, A.L. Beyer, *Methods Enzymol.* 180 (1989) 481–509.
- [45] O. Medalia, A.J. Koster, A. Tocilij, M. Angenitzki, J. Sperling, Z. Berkovitch-Yellin, R. Sperling, *J. Struct. Biol.* 120 (1997) 228–236.
- [46] C.W. Akey, M. Radermacher, *J. Cell Biol.* 122 (1993) 1–19.
- [47] T.D. Allen, J.M. Cronshaw, S. Bagley, E. Kiseleva, M.W. Goldberg, *J. Cell Sci.* 113 (2000) 1651–1659.
- [48] D.P. Bazett-Jones, M.J. Hendzel, *Methods* 17 (1999) 188–200.
- [49] F.J. Iborra, D.A. Jackson, P.R. Cook, *J. Cell Sci.* 113 (2000) 291–302.
- [50] W. Meyer-Ilse, D. Hamamoto, A. Nair, S.A. Lelievre, G. Denbeaux, L. Johnson, A.L. Pearson, D. Yager, M.A. Legros, C.A. Larabell, *J. Microsc.* 210 (2000) 3395–3403.
- [51] S.H. Leuba, G. Yang, C. Roberts, B. Samori, K. van Holde, J. Zlatanova, *Proc. Natl. Acad. Sci. USA* 91 (1994) 11621–11625.
- [52] J. Zlatanova, S.H. Leuba, K. van Holde, *Biophys. J.* 74 (1998) 2554–2566.
- [53] A. Pombo, P.R. Cook, *Exp. Cell Res.* 229 (1996) 201–203.
- [54] J.M. Sogo, F. Thoma, *Methods Enzymol.* 170 (1989) 142–179.
- [55] M.W. Goldberg, T.D. Allen, *J. Cell Biol.* 119 (1992) 1429–1440.